

RESEARCH ARTICLE

10.1002/2014JD021705

Special Section:

Fast Physics in Climate Models: Parameterization, Evaluation, and Observation

Key Points:

- Techniques for cloud fraction and cloud albedo retrievals are compared
- Retrievals using 16 years of ground-based shortwave radiation measurements
- The comparison shows overall good agreement

Correspondence to:

Y. Xie,
Yu.Xie@nrel.gov

Citation:

Xie, Y., Y. Liu, C. N. Long, and Q. Min (2014), Retrievals of cloud fraction and cloud albedo from surface-based shortwave radiation measurements: A comparison of 16 year measurements, *J. Geophys. Res. Atmos.*, 119, 8925–8940, doi:10.1002/2014JD021705.

Received 28 FEB 2014

Accepted 21 JUN 2014

Accepted article online 25 JUN 2014

Published online 21 JUL 2014

Retrievals of cloud fraction and cloud albedo from surface-based shortwave radiation measurements: A comparison of 16 year measurements

Yu Xie^{1,2}, Yangang Liu¹, Charles N. Long³, and Qilong Min⁴

¹Brookhaven National Laboratory, Upton, New York, USA, ²National Renewable Energy Laboratory, Golden, Colorado, USA, ³Pacific Northwest National Laboratory, Richland, Washington, USA, ⁴Atmospheric Sciences Research Center, State University of New York at Albany, Albany, New York, USA

Abstract Ground-based radiation measurements have been widely conducted to gain information on clouds and the surface radiation budget. To examine the existing techniques of cloud property retrieval and explore the underlying reasons for uncertainties, a newly developed approach that allows for simultaneous retrievals of cloud fraction and cloud albedo from ground-based shortwave broadband radiation measurements, XL2013, is used to derive cloud fraction and cloud albedo from ground-based shortwave broadband radiation measurements at the Department of Energy Atmospheric Radiation Measurement Southern Great Plains site. The new results are compared with the separate retrieval of cloud fraction and cloud albedo using Long2006 and Liu2011, respectively. The retrievals from the broadband radiation measurements are further compared with those based on shortwave spectral measurements (Min2008). The comparison shows overall good agreement between the retrievals of both cloud fraction and cloud albedo, with noted differences, however. The Long2006 and Min2008 cloud fractions are greater on average than the XL2013 values. Compared to Min2008 and Liu2011, the XL2013 cloud albedo tends to be greater for thin clouds but smaller for thick clouds, with the differences decreasing with increasing cloud fraction; the neglect of land surface albedo and cloud absorption by Liu2011 also contributes the difference in cloud albedo. Further analysis reveals that the approaches that retrieve cloud fraction and cloud albedo separately may suffer from mutual contamination of errors in retrieved cloud fraction and cloud albedo.

1. Introduction

One of the challenges in the general circulation models (GCMs) is the difficulty to represent subgrid processes/properties, e.g., cloud formation and dissipation, within a large-scale model grid box [Wigley *et al.*, 1990; Wyant *et al.*, 2006]. An accurate parameterization of cloud microphysical and macrophysical properties is required by the modeling of cloud climatology and climate variability. There has been a growing interest in utilization of available cloud property observations to evaluate the GCM cloud parameterizations and provide insights into error sources [Bouniol *et al.*, 2010; Hinkelman *et al.*, 1999; Hogan *et al.*, 2001a; Paquin-Ricard *et al.*, 2010; Sengupta *et al.*, 2004; Song *et al.*, 2013].

It is well known that the parameterization of cloud albedo represents integrals over many cloud properties, such as cloud particle size, and liquid and ice water contents [Han *et al.*, 1998]. Due to the limited spatial resolution of the GCMs, an accurate estimation of cloud fraction in each grid box is also required by the cloud parameterization [Hogan *et al.*, 2001b]. A number of studies have been performed to understand the role of cloud fraction and cloud albedo in the radiative transfer within the Earth-atmosphere system [Betts and Viterbo, 2005; Charlock and Ramanathan, 1985; Liu *et al.*, 2011]. Liu *et al.* [2011] reported a theoretical relationship between cloud albedo, cloud fraction, and cloud radiative forcing widely used in the evaluation of cloud feedback [Charlock and Ramanathan, 1985; Gautier and Landsfeld, 1997; Zhang *et al.*, 2012].

Progress has been made in the retrieval of cloud fraction and cloud albedo from long-term ground-based measurements such as those provided by the U.S. Department of Energy's Atmospheric Radiation Measurement (ARM) Program [Qian *et al.*, 2012]. In a series of papers by Dong *et al.* [2005, 2006], ground-based Eppley precision spectral pyranometer and lidar-radar measurements over the ARM Central Facility were used in a study of the climatology of cloud properties including cloud/top-of-atmosphere albedos and

cloud fraction associated with single-layer low, middle, and high clouds. *Kennedy et al.* [2013] compared 14 years of ARM Southern Great Plains (SGP) observations of cloud fraction from the Millimeter Cloud Radar, Micropulse Lidar, and Belfort/Vaisala Ceilometers in order to understand the impact of instrument on the estimation of cloud properties.

Compared to cloud measurements from millimeter cloud radars and lidars, ground-based shortwave (SW) radiation is commonly provided by worldwide surface observation stations and yet has the ability to extract valuable information on cloud fraction and cloud albedo [McFarlane et al., 2013; Ohmura et al., 1998]. Long et al. [2006, hereinafter Long2006] reported a retrieval of fractional sky cover on the basis of broadband SW measurements from the National Oceanographic and Atmospheric Administration Surface Radiation Research Branch (SRRB) near Boulder, Colorado, and ARM Climate Research Facility (ACRF) SGP site. The determined fractional sky cover at the ARM SGP site was used by Liu et al. [2011, hereinafter Liu2011] to infer cloud albedo through the computation of SW relative cloud radiative forcing (RCRF) at the surface. Min et al. [2008, hereinafter Min2008] proposed a ratio method to estimate cloud fraction using spectral radiation measurements from a pair of multifilter rotating shadowband radiometer (MFRSR) channels at 0.415 and 0.86 μm . Xie and Liu [2013, hereinafter XL2013] extended the study of Liu2011 and derived the analytical solutions of cloud fraction and cloud albedo from the downwelling total and direct SW fluxes measured at the land surface. The simultaneous retrievals of cloud fraction and cloud albedo eliminate the mutual contamination of errors from the separate retrievals if any.

The purpose of this study is to examine these different approaches for retrieving cloud fraction (Long2006, Min2008, and XL2013) and cloud albedo (Min2008, Liu2011, and XL2013), quantify the differences between the retrievals, explore the underlying reasons/assumptions for the differences, and understand how these underlying reasons/assumptions affect the cloud retrievals by the different approaches. To accomplish this goal, we analyze and compare retrievals using 16 years (1997–2012) of ground-based measurements of SW radiation. The rest of the paper is organized as follows. Section 2 describes the radiation measurements and retrieval techniques to determine cloud fraction and cloud albedo. In section 3, a long-term comparison of the retrieved cloud fraction and cloud albedo from 1997 to 2012 is presented. Section 4 analyzes the underlying mechanisms related to the differences among difference retrievals. The conclusions of this study and future work are discussed in section 5.

2. Description of Radiation Measurements and Retrieval Algorithms

The SW direct and diffuse radiation is measured by the Solar Infrared Radiation Station (SIRS) radiometers mounted on a solar tracker. The SIRS radiometers operate in broadband SW and longwave channels between 0.3–3.0 μm and 4.0–50.0 μm , respectively, and provide continuous measurements of upwelling and downwelling radiation, allowing the study of the long-term surface radiative flux exchange at the ARM SGP site. The SW radiative fluxes used in the retrieval of cloud fraction and cloud albedo are provided by the Shortwave Flux Analysis (SWFA) value-added product (VAP) in a 15 min temporal resolution [Long and Ackerman, 2000; Long and Gaustad, 2004; Long et al., 2006]. The clear-sky SW radiative flux from the SWFA VAP is estimated by an empirical fitting algorithm along with a series of tests determining cloud conditions [Long and Ackerman, 2000].

The spectral radiative fluxes are taken by the MFRSR that uses independent interference-filter-photodiode detectors and the automated rotating shadowband technique to provide spectral measurements. The total, direct, and diffuse radiative fluxes over ARM SGP site are available in spectral channels centered near 0.415, 0.5, 0.61, 0.86, and 0.94 μm [Harrison et al., 1994]. Solar constant is extrapolated from Langley regression with radiative fluxes measured over clear sky. The diffuse transmittance can be subsequently computed from all-sky-measured flux normalized by solar constant. Thus, transmittance ratio, representing the ratio of diffuse transmittances in two spectral channels, is independent of data calibration, ensuring better accuracy compared to other measurements of radiative properties. Cloud fraction is then retrieved using transmittance ratio in a 5 min temporal resolution and aggregated to match the temporal resolution (15 min) of the SWFA data.

The rest of this section briefly introduces the different retrieval approaches. Details are referred to the original papers reporting these approaches [Liu et al., 2011; Long et al., 2006; Min et al., 2008; Xie and Liu, 2013].

2.1. Determination of Cloud Fraction Based on Long2006

Cloud fraction from the SWFA VAP is essentially derived on the basis of Long2006. The SW radiation at the surface is first screened by diffuse ratio and diffuse cloud effect defined as

$$D_r = \frac{F_{all,u}^{dn}}{F_{all}^{dn}} \tag{1a}$$

$$D_n = \frac{F_{all,u}^{dn} - F_{clr,u}^{dn}}{F_{clr}^{dn}} \tag{1b}$$

where F_{all}^{dn} and F_{clr}^{dn} are the downwelling flux for all and clear skies, respectively, and the second subscript u indicates that the corresponding quantities are for diffuse radiation. The overcast clouds and clear-sky periods are identified according to the magnitude and variability of D_r and D_n and a procedure reported by Long and Ackerman [2000]. The cloud fraction, f , in the remaining data is estimated using an empirical equation obtained by curve fitting the relationship between the hemispheric sky imager data at SRRB and ACRF and D_n :

$$f = 2.225D_n^{0.9381} \tag{2}$$

Note that the common definition of cloud fraction is nadir-projected cloud amount, i.e., the amount of cloud shadow on the ground divided by the total area of the ground. However, that estimated by Long2006 is related to the amount of the sky view that contains cloud elements divided by the total hemispheric angular view, and thus normally referred to as fractional sky cover. Kassianov *et al.* [2005] compared cloud fraction and fractional sky cover in both computational models and surface-based measurements. It was found that fractional sky cover tends to be greater than cloud fraction due to the line-of-site loss of view of the clear area interspersed between the broken clouds as the view nears the horizon when the intercloud spaces are not affected in terms of nadir-projected cloud fraction. The difference between hemispheric sky cover and nadir-projected cloud fraction can reach up to $\pm 50\%$ cloud fraction in instantaneous sky cover retrievals depending on where in the sky view the cloudiness resides [Henderson-Sellers and Mcguffie, 1990]. Kassianov *et al.* [2005] showed that a 15 min average of highly sampled sky cover (1 min resolution or better) effectively mitigates this instantaneous sample discrepancy, producing an average that much closely relates to cloud fraction with only the residual positive bias associated with loss of line-of-sight of the gaps between clouds nearer the horizon in the sky view. This positive bias compared to nadir-projected cloud fraction is on average greatest for sky cover values of 50% and decreases to zero for clear and overcast skies. Thus, the 15 min averaged fractional sky cover provided by Long2006 provides a reasonable estimation of cloud fraction for our purposes [Kassianov *et al.*, 2005]. For convenience, fractional sky cover is referred to as cloud fraction in the rest of this paper. The uncertainty related to the geometry in the observations will be further discussed in section 4.

2.2. Determination of Cloud Albedo Based on Liu2011

Liu2011 developed an algorithm to derive cloud albedo using the radiation measurement from SWFA VAP including the previously determined cloud fraction based on Long2006. Briefly, for an overcast single-layer cloud over a black land surface, the downwelling flux scattered by the cloud can be given by

$$F_{cld}^{dn} = (1 - \alpha)F_{clr}^{dn} \tag{3a}$$

$$\alpha = \alpha_r + \alpha_a \tag{3b}$$

where α_r and α_a are cloud albedo and cloud absorption, respectively. The all-sky downwelling flux is simplified by equations (3a) and (3b) assuming $\alpha_a = 0$:

$$\begin{aligned} F_{all}^{dn} &= fF_{cld}^{dn} + (1 - f)F_{clr}^{dn} \\ &= (1 - \alpha_r)fF_{clr}^{dn} + (1 - f)F_{clr}^{dn} \end{aligned} \tag{4a}$$

The relative cloud radiative forcing (RCRF) (Betts [2007] called it effective cloud albedo) is used in the derivation:

$$\alpha_{cld}^{SRF} = 1 - \frac{F_{all}^{dn}}{F_{clr}^{dn}} \tag{4b}$$

Substituting equation (4b) into equation (4a) yields the following:

$$\alpha_r = \frac{\alpha_{cld}^{SRF}}{f} \tag{4c}$$

Cloud albedo is retrieved by applying to equation (4c) $\alpha_{\text{cd}}^{\text{SRF}}$, estimated surface measurements of radiative flux, and cloud fraction estimated with the Long2006 approach.

2.3. Determination of Cloud Fraction and Cloud Albedo Based on Min2008

Min2008 investigated surface measurements of transmittance ratio (TR) defined by

$$\text{TR} = \frac{F_{u,860}^{\text{dn}}}{F_{u,415}^{\text{dn}}} \quad (5)$$

where $F_{u,415}^{\text{dn}}$ and $F_{u,860}^{\text{dn}}$ represent diffuse radiative fluxes at 0.415 and 0.86 μm , respectively. The observed transmittance ratio is sensitive to cloudy- or clear-sky conditions and can be assumed as a linear partition between their transmittance ratios:

$$\text{TR}_{\text{all}} = (1 - f)\text{TR}_{\text{clr}} + f\text{TR}_{\text{cld}} \quad (6a)$$

Thus, cloud fraction is derived from equation (6a) as follows:

$$f = \frac{\text{TR}_{\text{all}} - \text{TR}_{\text{clr}}}{\text{TR}_{\text{cld}} - \text{TR}_{\text{clr}}} \quad (6b)$$

The clear-sky transmittance ratio is given as 0.3 on the basis of the mean value of the measurements when cloud optical thickness is smaller than 0.01. The cloudy-sky transmittance ratio, proved insensitive to cloud optical thickness when it is greater than 6, is approximated by measurements associated with large cloud optical thicknesses and given as 1.38 following the minimum value during overcast thick cloud period.

For cloud overcast condition, cloud optical thickness is retrieved by comparing measured and computed cloudy-sky atmospheric transmittance at the spectral wavelengths of MFRSR as described by *Min and Harrison* [1996]. For broken clouds, cloud optical thickness is determined from the direct beam component of the spectral fluxes with forward scattering correction [*Min et al.*, 2004]. For comparison, the optical thickness is converted to cloud albedo using the relationship between cloud albedo and cloud optical thickness as described in XL2013.

2.4. Simultaneous Retrieval of Cloud Fraction and Cloud Albedo Based on XL2013

XL2013 reported a simultaneous retrieval of cloud fraction and cloud albedo using the surface measurements of total and direct radiative fluxes. When the multiple reflections between cloud and land surface are taken into account, the total downwelling and upwelling radiative fluxes can be given by

$$F_{\text{all}}^{\text{dn}} = F_1 (1 - \alpha_s \alpha_r f T^2)^{-1} \quad (7a)$$

$$F_{\text{all}}^{\text{up}} = F_1 \alpha_s (1 - \alpha_s \alpha_r f T^2)^{-1} \quad (7b)$$

where α_s and T are land surface albedo and the transmittance of the atmosphere under the cloud for diffuse radiation, respectively. F_1 is the first-order downwelling flux at surface and can be written as

$$F_1 = f F_{\text{cld}}^{\text{dn}} + (1 - f) F_{\text{clr}}^{\text{dn}} \quad (7c)$$

A combination of equations (3a), (3b), and (7a)–(7c) leads to

$$f = \frac{F_{\text{clr}}^{\text{dn}} - F_{\text{all}}^{\text{dn}}}{\alpha F_{\text{clr}}^{\text{dn}} - \alpha_r F_{\text{all}}^{\text{up}} T^2} \quad (7d)$$

For direct radiation, the downwelling flux is given by

$$F_{\text{all},d}^{\text{dn}} = f F_{\text{cld},d}^{\text{dn}} + (1 - f) F_{\text{clr},d}^{\text{dn}} \quad (8a)$$

where the second subscript d indicates that the corresponding quantities are for direct radiation. $F_{\text{cld},d}^{\text{dn}}$ can be given according to the Beer-Lambert law for extinction:

$$F_{\text{cld},d}^{\text{dn}} = F_{\text{clr},d}^{\text{dn}} e^{-\tau/\mu_0} \quad (8b)$$

where τ is the cloud optical thickness for the SW spectrum and μ_0 is the cosine value of solar zenith angle. A combination of equations (8a) and (8b) yields another equation for f :

$$f = \frac{F_{\text{clr},d}^{\text{dn}} - F_{\text{all},d}^{\text{dn}}}{F_{\text{clr},d}^{\text{dn}} (1 - e^{-\tau/\mu_0})} \quad (8c)$$

Table 1. Summary of the Retrieval Algorithms

Cloud Fraction			
	Long2006	Min2008	XL2013
Data	Broadband	Spectral	Broadband
Surface albedo	Considered	Considered	Considered
Simultaneous retrieval	No	No	Yes
Cloud Albedo			
	Liu2011	Min2008	XL2013
Data	Broadband	Spectral	Broadband
Surface albedo	No	Considered	Considered
Cloud absorption	No	Considered	Considered
Simultaneous retrieval	No	No	Yes

Then α_r and f can be simultaneously solved by equations (7d) and (8c) when α_a is neglected and a two-stream approximation suggested by *Sagan and Pollack* [1967] is used to simulate α_r from τ . The effect of cloud absorption is corrected later using the Rapid Radiative Transfer Model [Mlawer et al., 1997; Oreopoulos and Barker, 1999] and a suite of numerical experiments.

The major features of the above mentioned retrieval algorithms can be found in Table 1.

3. Long-Term Comparison of Cloud Fraction and Cloud Albedo Retrievals

To understand the difference between the retrievals by Long2006, Min2008, Liu2011, and XL2013, we compared cloud fractions and cloud albedos using 16 years data from the SWFA VAP and MFRSR during 25 March 1997 to 21 September 2012. The cloud fractions and cloud albedos are either provided by the data or retrieved using measurements of surface-based radiative fluxes. Figure 1a shows the comparison of cloud fraction between Long2006 and XL2013 when the retrievals of Long2006, Min2008, and XL2013 are available. The color in the figure represents normalized density of the data including a total of 69,125 scenarios. The cloud fractions related to Long2006 are directly taken from SWFA VAP. As most of the cloud albedo retrievals by Min2008 are missing when cloud fraction is smaller than 0.2, the comparison is performed when cloud fraction is identified as between 0.2 and 1.0 by Long2006, Min2008, and XL2013. Thus, the comparisons below represent 53.5% of the retrievals when they are available by both Long2006 and XL2013. It can be inferred from Figure 1a that the cloud fractions from the two retrieval algorithms have a reasonable agreement. The least squares fitting (red line) indicates overall smaller cloud fractions estimated by XL2013. The relative difference of cloud fractions between Long2006 and XL2013 attenuates when $f(\text{Long2006}) > 0.5$ and $f(\text{Long2006}) < 0.2$ (not shown here due to the limited retrieval by Min2008).

Min2008 and XL2013 also show a generally good agreement except for clouds when cloud fraction is large (Figure 1b). It is noticeable that Min2008 identifies more cloud overcast conditions compared to XL2013 and Long2006.

Note that the differences of the cloud fractions in the above discussion are smaller than the spread of general products. For instance, *Wu et al.* [2014] examined cloud fractions by surface- and satellite-based measurements over the ARM SGP site from 1997 to 2011. It revealed that the annually averaged cloud fractions from the Active Remote Sensing of Clouds and International Satellite Cloud Climatology Project are 0.08–0.10 larger than surface-based retrievals, larger than the difference between Long2006, Min2008, and XL2013 considering the exclusion of small cloud fractions. Nevertheless, this paper focuses on the differences in order to further improve the retrievals.

Compared to cloud fraction, the available products of cloud albedo and intercomparisons are even more limited. Figure 1c compares cloud albedos retrieved with Liu2011 and XL2013 for the same cases as Figures 1a and 1b. For thin clouds (e.g., $\alpha_r(\text{Liu2011}) < 0.4$), cloud albedos retrieved by XL2013 are larger than Liu2011. Their relative difference decreases with increasing cloud albedo and becomes negative when the cloud is thick (e.g., $\alpha_r(\text{Liu2011}) > 0.4$). The Liu2011 retrieval overestimates the cloud albedos for the thick clouds by ~5%. The overestimation is likely related to the neglected cloud absorption in Liu2011, because both forward and backward scattering by the cloud increase when cloud absorption is not accounted in the simulation of radiative transfer within clouds. As expected, the absorption impact becomes more important with the increase of cloud optical thickness. It is also found in Figure 1c that the disagreement in cloud albedos for thick clouds between XL2013 and Liu2011 is larger compared to that caused by the neglect of cloud absorption; further discussion on the possible reasons is deferred to the next section. For thin clouds, the disagreement between Liu2011 and XL2013 is likely related to land surface albedo and mutual contamination of errors which can be also found in the next section. Compared to the cloud albedo based on Min2008 (Figure 1d),

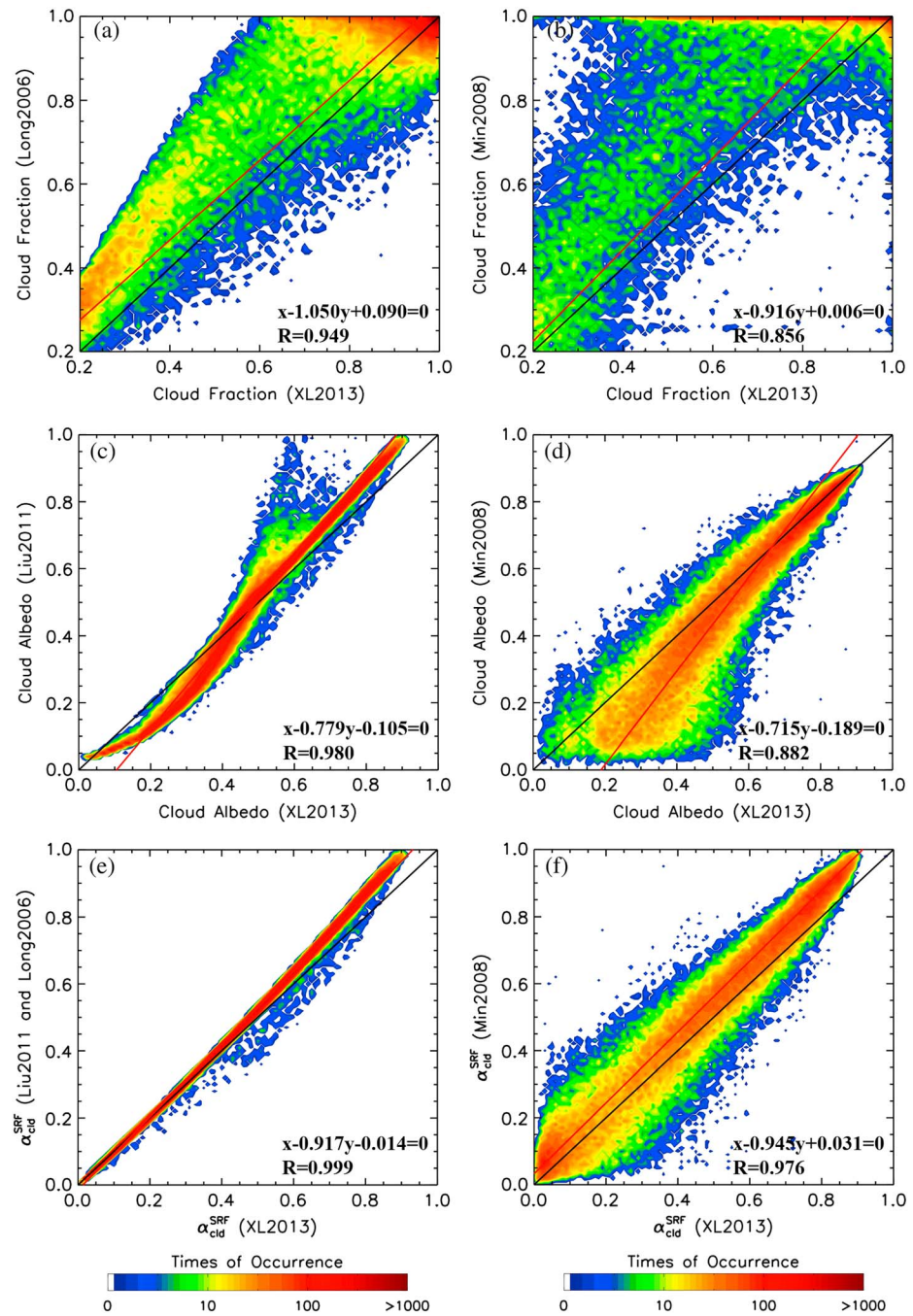


Figure 1. Comparison of (a) cloud fractions from Long2006 and XL2013, (b) cloud fraction from Min2008 and XL2013, (c) cloud albedos from Liu2011 and XL2013, (d) cloud albedos from Min2008 and XL2013, (e) RCRFs from Liu2011 and Long2006, and XL2013, and (f) RCRFs from Min2008 and XL2013. The red and black lines are associated with a least squares fit to all data and perfect match, respectively. The equations of the fitting curve (red line) and its R value are given in each panel.

cloud albedo from XL2013 is larger when cloud albedo is small, but gradually agrees with Min2008 for thicker clouds. This trend is similar to cloud 3-D effect which becomes less important with the increase of cloud optical thickness and horizontal dimension, suggesting a possible 3-D effect on retrievals.

The retrievals of cloud fraction and cloud albedo can be further understood by examining the RCRF computed using equation (4c) and that derived from the retrieved cloud fraction and cloud albedo

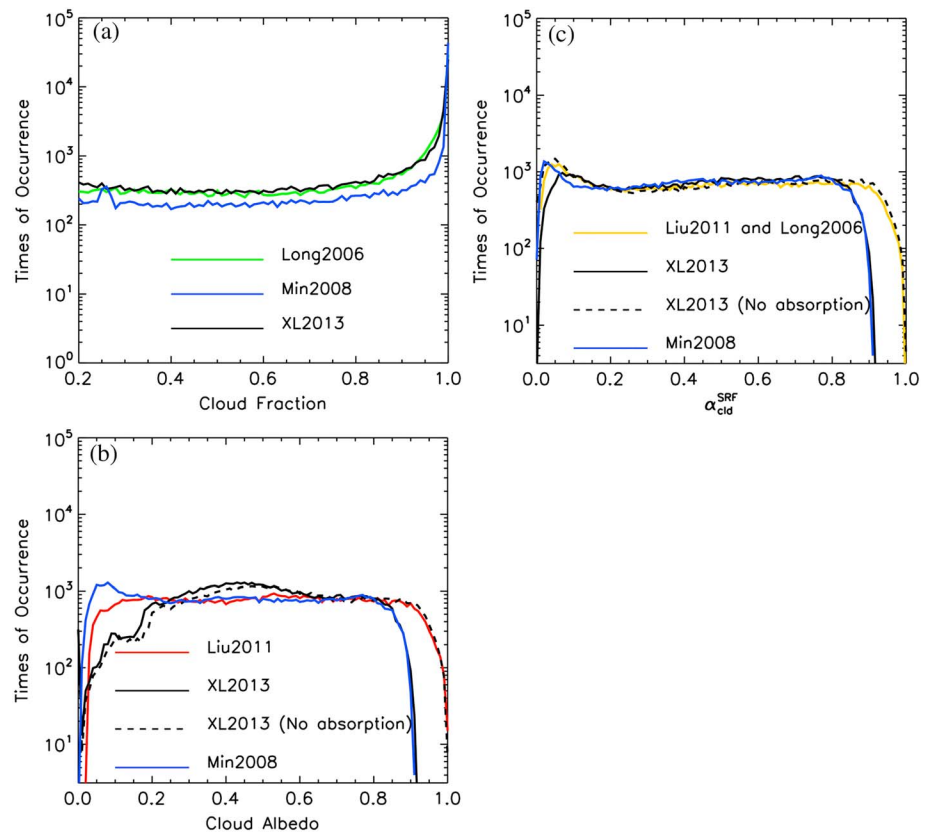


Figure 2. Histograms of (a) cloud fractions from Long2006, Min2008, and XL2013, (b) cloud albedos from Liu2011, Min2008, and XL2013, and (c) RCRFs from Liu2011 and Long2006, Min2008, and XL2013. Note that the comparisons are presented on a logarithmic scale.

(see Figures 1e and 1f). It is seen that the RCRFs from XL2013, Min2008, Liu2011, and Long2006 have excellent agreement. Similar to cloud albedo, the slight differences of Figure 1e when $\alpha_{\text{clid}}^{\text{SRF}} > 0.5$ correspond to the correction of cloud absorption by XL2013. Compared to the derivation of RCRF by Liu2011 and XL2013, the slightly smaller values by Liu2011 are related to the neglect of land surface albedo.

The excellent agreement of the RCRFs indicates that the smaller cloud fractions based on XL2013 are associated with the greater cloud albedos compared to Liu2011 and Min2008. The cloud albedos from the algorithms should have a better agreement for cases with similar cloud fractions.

Figure 2 illustrates the histograms of the retrievals shown in Figure 1. In Figure 2a, the cloud fractions from Long2006, Min2008, and XL2013 show similar probability distributions. Compared to Long2006 and XL2013, Min2008 provides more overcast retrievals where they are dense from all the algorithms. The comparison of cloud albedos (Figure 2b) indicates that Liu2011 produces more thick clouds than XL2013. The difference in the thick clouds is likely caused by cloud absorption neglected by Liu2011 because the agreement between two retrievals becomes better when cloud absorption is neglected in XL2013. The cloud absorption also explains the difference of RCRF in Figure 2c. Compared to the neglect of cloud absorption, other factors seem to have secondary impacts on the simulation of RCRF.

Figure 3 illustrates the diurnal, annual, and interannual variations of cloud fraction and cloud albedo during 1997–2012. From Figure 3a, the average of cloud albedos peaks at ~6:00 and reaches a minimum at ~12:00. The cloud albedos of Min2008 and Liu2011 increase from 12:00 to 18:00 while those of XL2013 decrease through 18:00. The difference between XL2013 and Liu2011 peaks at 12:00 and 18:00 suggesting a larger amount of thin cloud occurrence based on Figure 1c. The monthly and annually mean cloud albedos in Figures 3b and 3c show slight difference between Liu2011 and XL2013 and variations with an overall average of ~0.6. Among the three panels, cloud albedos from Min2008 are associated with the smallest values.

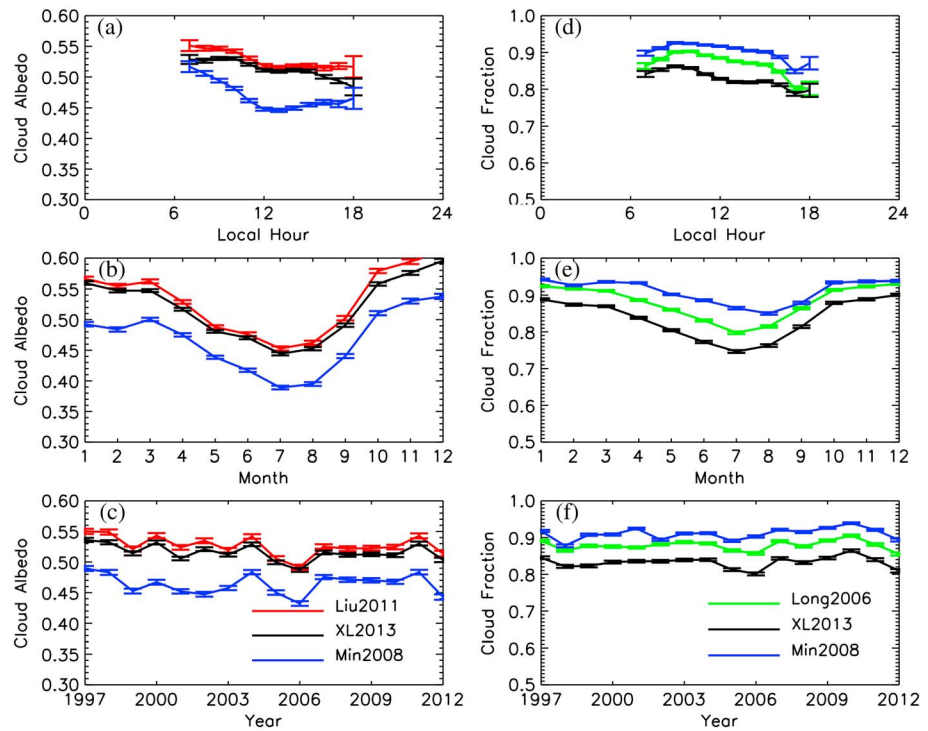


Figure 3. Diurnal, annual, and interannual variations of cloud fraction and cloud albedo. The error bars represent the standard errors of the retrieved cloud albedos and cloud fractions.

Hourly mean cloud fraction in Figure 3d decreases from ~10:00 to 18:00 for all methods. The overall smaller cloud fractions of XL2013 match the comparison of Figures 1a and 1b. Monthly mean cloud fractions are shown in Figure 3e where the peaks and troughs occur during January and July, respectively. The monthly mean cloud fractions of XL2013 have the same pattern to Long2006 and Min2008 but lower values. The overall mean cloud fractions of Long2006, Min2008, and XL2013 are 0.882, 0.911, and 0.837, respectively. According to other surface and satellite observations around ARM SGP site, the overall mean cloud fraction varies from 0.48 to 0.50 [Dong et al., 2006; Lazarus et al., 2000; Warren et al., 1986]. The greater average cloud fractions by Long2006, Min2008, and XL2013 are related to many invalid retrievals by Min2008 which are identified as clear sky by both Long2006 and XL2013, thus are eliminated from this data set. Similar to Figure 3e, the annual mean cloud fraction of XL2013 also shows a same pattern to Long2006 and Min2008 with slightly smaller values.

The monthly mean cloud fractions and cloud albedos from surface-based retrievals are further compared to those based on the Geostationary Operational Environmental Satellite 8/11 measurements on a $0.5^\circ \times 0.5^\circ$ grid over the ARM SGP domain (see Figure 4) [Minnis et al., 2008]. The comparison involves 3120 scenarios of 15 min data when both surface- and satellite-based retrievals are available. It can be seen from Figure 4a that the surface-based retrievals of cloud fraction are greater than satellite retrievals which have the best agreement to XL2013. The surface-based retrievals of cloud albedo, however, are smaller than satellite retrievals as can be found in Figure 4b.

4. Further Analysis

4.1. Theoretical Comparison of Long2006, Min2008, Liu2011, and XL2013

To theoretically understand the difference between Long2006, Min2008, Liu2011, and XL2013, we first analyze the empirical formulation of equation (2) using the quantities that can be measured at the surface. When land surface albedo is negligible, $F_{all,u}^{dn}$ can be given by

$$F_{all,u}^{dn} = fF_{cl,u}^{dn} + (1 - f)F_{clr,u}^{dn} \tag{9a}$$

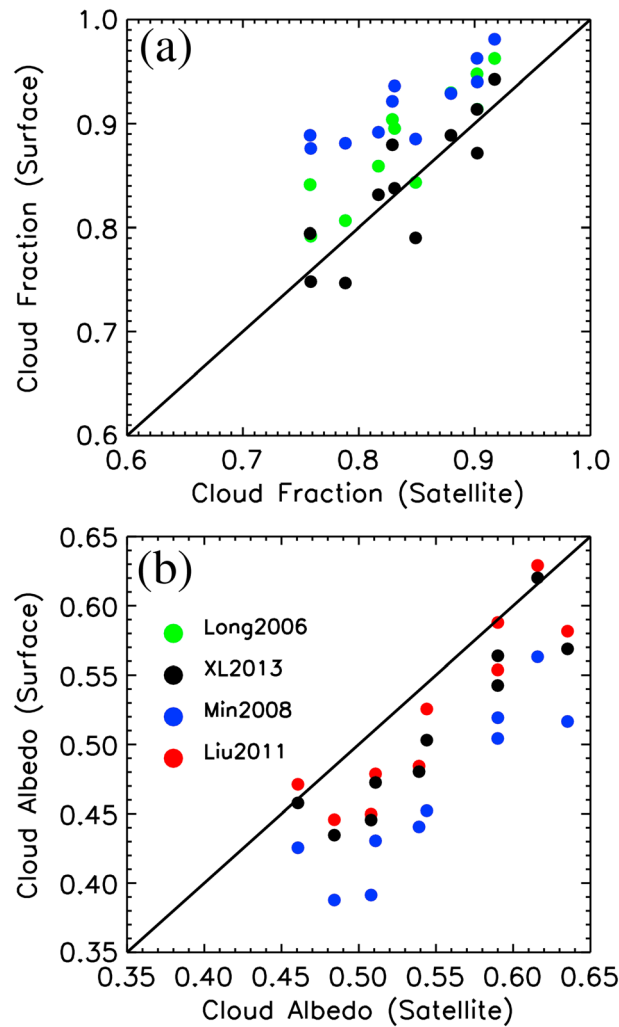


Figure 4. Comparison of (a) cloud fractions and (b) cloud albedos derived using surface- and satellite-based retrieval algorithms. The cloud fractions and cloud albedos are monthly averaged during 1997–2012 when the retrievals are provided by all the algorithms.

retrieved cloud albedo from Liu2011 is not utilized by Long2006 to improve the accuracy of cloud fraction though Long2006 has a good agreement to sky imager retrievals. In other words, the separate retrieval of cloud fraction and cloud albedo may lead to mutual contamination of errors. Similar uncertainty may exist in Min2008 when cloud is thin because the cloudy-sky transmittance ratio in equation (6b) is an empirical value for thick clouds.

Compared to Long2006, Min2008, and Liu2011, XL2013 has overcome this uncertainty by simultaneously retrieving the cloud fraction and cloud albedo. Unlike Long2006, XL2013 uses the same algorithm to determine the cloud fraction for all scenarios including clear-sky and overcast cloud. Compared to Liu2011, the simulation of the radiative transfer is also improved by considering land surface albedo and cloud absorption.

4.2. Effect of Land Surface Albedo and Cloud Absorption

Based on the discussion of section 2, land surface albedo, α_s , over the ARM SGP area affects the measurement of $F_{all,u}^{up}$ and therefore the retrieval of cloud fraction and cloud albedo by XL2013 through equation (7d). In the algorithm of Long2006, retrieved cloud fraction is a function of land surface albedo due to the use of $F_{all,u}^{dn}$ in equation (1b) [Long and Ackerman, 2000]. The diffuse radiative flux measured at the land surface ($F_{all,u}^{dn}$) is a total

Following equation (9a), cloud fraction can be expressed by

$$f = \frac{F_{all,u}^{dn} - F_{clr,u}^{dn}}{F_{cld,u}^{dn} - F_{clr,u}^{dn}} = \frac{F_{clr}^{dn}}{F_{cld,u}^{dn} - F_{clr,u}^{dn}} D_n \quad (9b)$$

To simplify the derivation, we ignore scattering by aerosols and air molecules in the atmosphere indicating $F_{clr,u}^{dn} = 0$. Then equation (9b) can reduce to

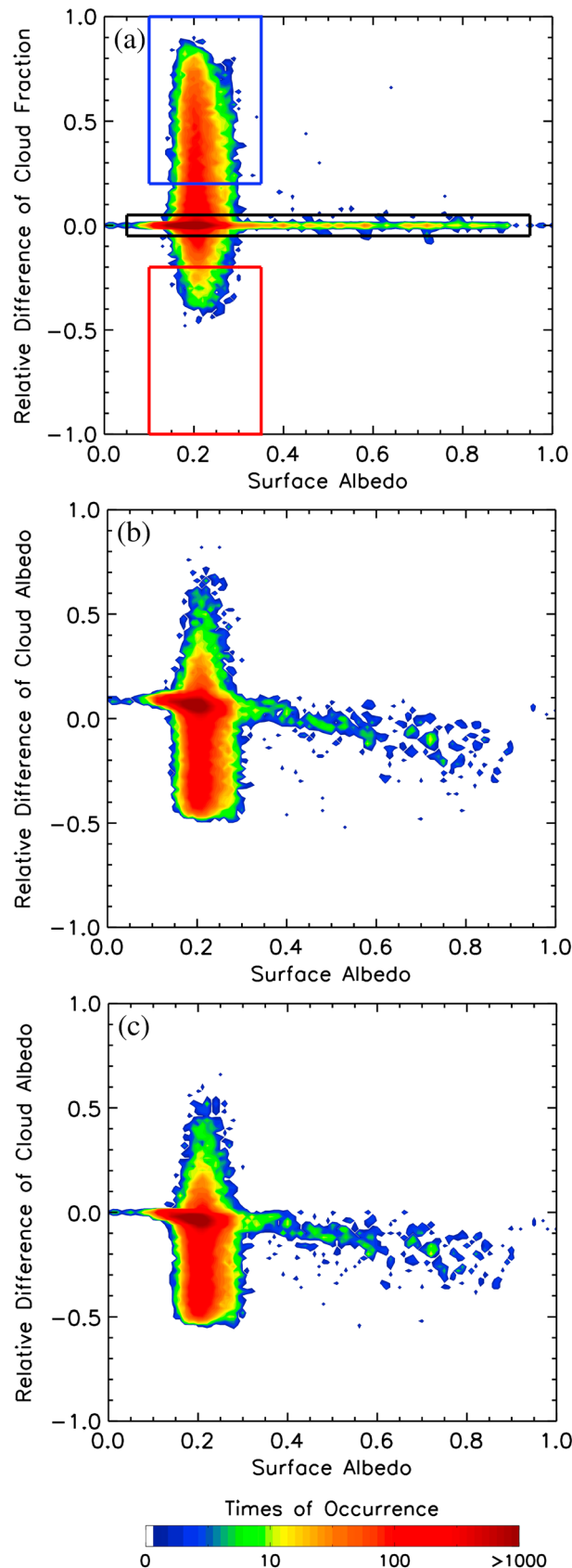
$$f = \frac{F_{clr,d}^{dn}}{F_{cld}^{dn} - F_{cld,d}^{dn}} D_n \quad (9c)$$

With equations (3a), (3b), and (8b), equation (9c) can be further simplified to get

$$f = \frac{D_n}{1 - \alpha - e^{-\tau/\mu_0}} \quad (9d)$$

It is clear from equation (9d) that D_n should be a function of f and α_r since α and τ/μ_0 are functions of α_r . However, D_n in the empirical formulation of equation (2) is only related to f , which indicates the neglect of cloud albedo in the retrieval of cloud fraction. Note that surface albedo and clear-sky diffuse flux are nonzero in Long2006 creating a complex relationship between D_n , cloud albedo, and cloud fraction. However, D_n is still determined by both cloud albedo and cloud fraction.

From the derivation above, it is also obvious that the absence of accounting cloud albedo variability causes uncertainty in the determination of cloud fraction (by Long2006), which in turn affects the retrieval of cloud albedo (by Liu2011). The



of diffused solar flux after scattered by cloud and that associated with multiple reflection between cloud and land surface. Thus, $F_{all,u}^{dn}$ is dependent on land surface albedo, which becomes more obvious with the increase of cloud fraction and cloud albedo. For the retrieval of cloud fraction by Min2008, land surface albedo affects the measurements of transmittance ratio. In the retrieval of cloud albedo by Liu2011, land surface albedo is ignored to circumvent the complex derivation of the multiple reflections between cloud and land surface. Due to the different use of land surface albedo in solving the radiative transfer process, it is first useful to examine the impact of land surface albedo on the differences in the retrievals.

Figure 5 shows the relative difference of cloud fraction (RDF) and relative difference of cloud albedo (RDA) between Long2006 and XL2013 as functions of land surface albedo, computed by the ratio of upward to downward total fluxes for clear-sky condition. It can be found that most of the cloud observations take place when $0.15 < \alpha_s < 0.35$, corresponding to the typical range of surface conditions over the ARM SGP area. A peak of RDF appears around the zero-basis field in Figure 5a indicating a general good agreement between Long2006 and XL2013. As the surface albedo is considered in both retrievals, we expected the insensitivity of RDF to surface albedo, which is suggested by Figure 5a where the means in RDF are near zero with increasing surface albedo. In contrast to RDF, land surface albedo has small but visible impact on the retrieving difference between Liu2011 and XL2013 (see Figure 5b). The fact that the surface albedo in Liu2011 is omitted but not in XL2013 suggests that the surface albedo contributes to the nonzero in the mean

Figure 5. (a) RDFs $\left(\frac{f(\text{Long2006}) - f(\text{XL2013})}{f(\text{XL2013})}\right)$, (b) RDAs $\left(\frac{\alpha_c(\text{Liu2011}) - \alpha_c(\text{XL2013})}{\alpha_c(\text{XL2013})}\right)$, and (c) RDAs when cloud absorption is not accounted by XL2013 as functions of surface albedo. The blue, black, and red boxes are corresponding to the areas where $0.2 < \text{RDF} < 1.0$ and $0.1 < \alpha_s < 0.35$, $-0.05 < \text{RDF} < 0.05$ and $0.05 < \alpha_s < 0.95$, and $-1.0 < \text{RDF} < -0.2$ and $0.1 < \alpha_s < 0.35$, respectively.

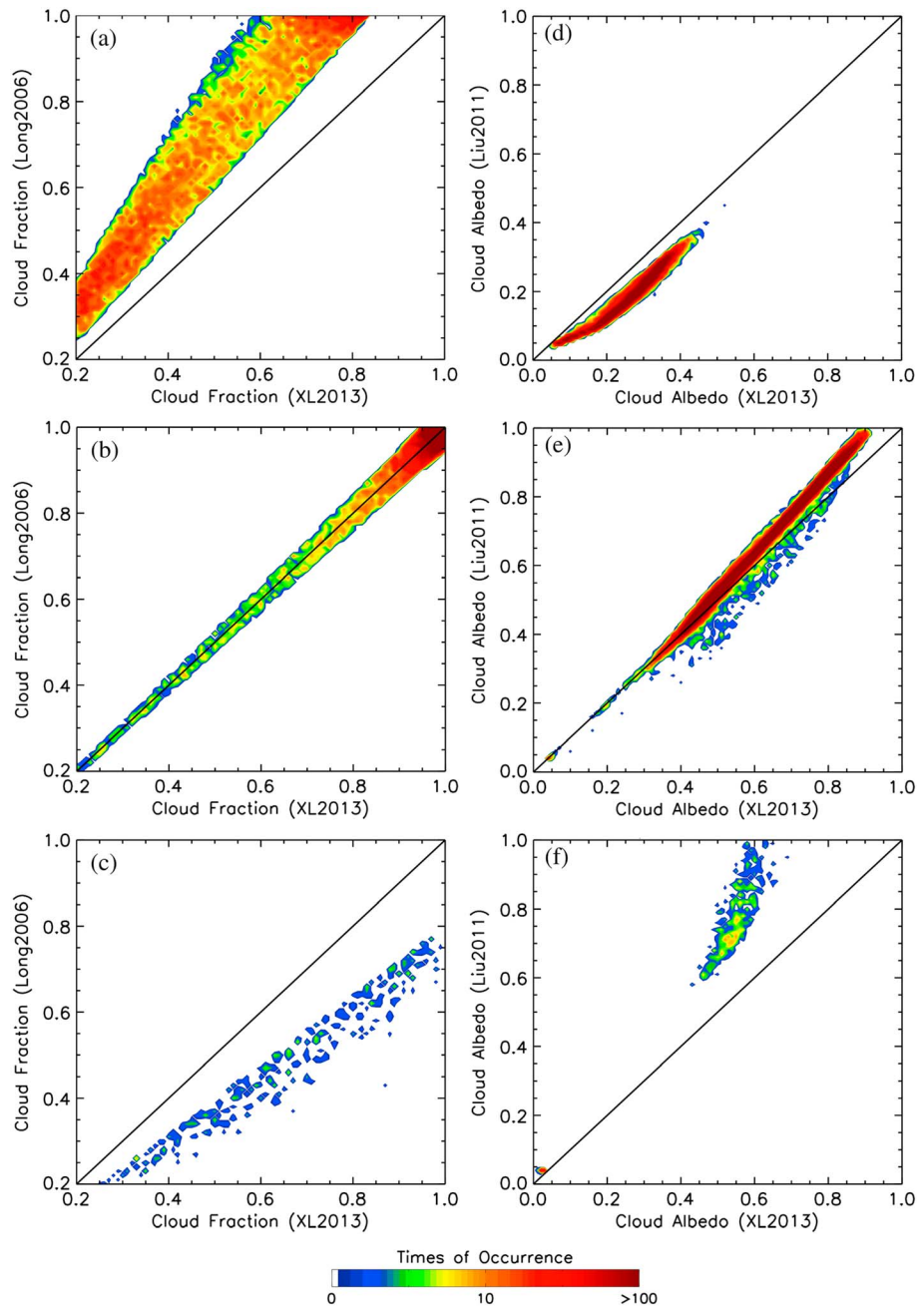


Figure 6. (a–c) Comparisons of cloud fractions from Long2006 and XL2013 for observations in the blue, black, and red boxes of Figure 5a, respectively, and (d–f) those of cloud albedos from Liu2011 and XL2013.

RDA, and the RDA becomes more pronounced when the land surface albedo becomes larger. As the observations associated with large land surface albedo are rare over the ARM SGP site, this uncertainty should be limited compared to other factors.

In addition to land surface albedo, cloud absorption is also ignored by Liu2011, which may cause a 5–13% overestimation of cloud albedo based on the discussion of XL2013. In XL2013, cloud absorption is taken into account by employing an adjusting equation derived from the simulations using the rapid radiative transfer model with and without cloud absorption considered. Figure 5c is the same as Figure 5b except that cloud absorption is removed from XL2013. It is seen that the sense part of the RDA decreases is close to zero indicating a better agreement between Liu2011 and XL2013. Compared to a simultaneous retrieval of cloud

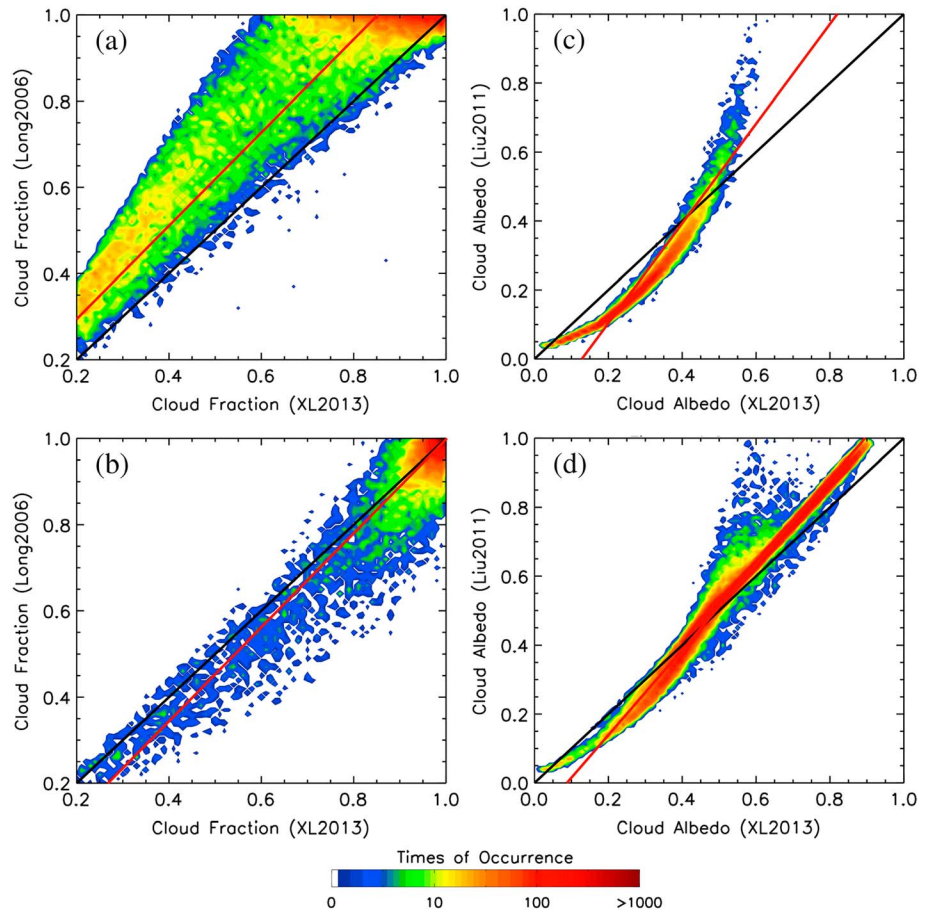


Figure 7. Comparison of cloud fraction when (a) $\alpha_r(\text{XL2013}) \leq 0.63$ and (b) $\alpha_r(\text{XL2013}) > 0.63$, and comparison of cloud albedo when (a) $f(\text{XL2013}) \leq 0.45$ and (b) $f(\text{XL2013}) > 0.45$. The red and black lines are associated with a least squares fit to all data and perfect match, respectively.

absorption with the determination of cloud fraction and cloud albedo, the corrected cloud absorption is affected by atmospheric absorption at the broadband SW wavelengths. Thus, the accuracy of the retrieval can be improved by using spectral measurements of radiation at minimal absorption wavelengths and compared with Min2008. Detailed discussion on this effect is available in XL2013.

4.3. Effect of Observational Conditions and Cloud Structures

The cloud fraction from Long2006 represents 15 min averages of hemispherical sky cover in a solid angle within a 160° field of view (FOV) [Long et al., 2006]. In XL2013, a plane-parallel cloud layer is assumed in the 15 min averaged retrieval of cloud fraction which can be approximated by nadir-view cloud fraction having an appropriate averaging time. Kassianov et al. [2005] examined the difference between the hemispherical and nadir-view cloud fractions caused by observational conditions and cloud structures. The hemispherical cloud fraction can be larger or smaller than that observed in the nadir direction when cloud is located in the center or edge of the FOV, respectively. Following the hemispherical observations during the ARM Program’s Cloudiness Intercomparison Intensive Operational Period, the temporal average over 15 min can efficiently eliminate the difference between narrow FOV (cone zenith angle $< 50^\circ$) hemispherical and nadir-view cloud fractions. However, the 160° FOV cloud fractions are almost nonexclusively greater than those in narrow FOV when they are small. The difference decreases with the increase of cloud fraction that can be described by a fitting function:

$$f(160^\circ) = 0.815 \times f(60^\circ) + 0.170 \quad (10)$$

where $f(160^\circ)$ and $f(60^\circ)$ represent 160° and 60° FOV cloud fractions, respectively. Thus, the relatively greater cloud fraction by Long2006 and Min2008 compared to XL2013 (Figures 1a and 1b) can be partially related to the observational conditions and cloud structures.

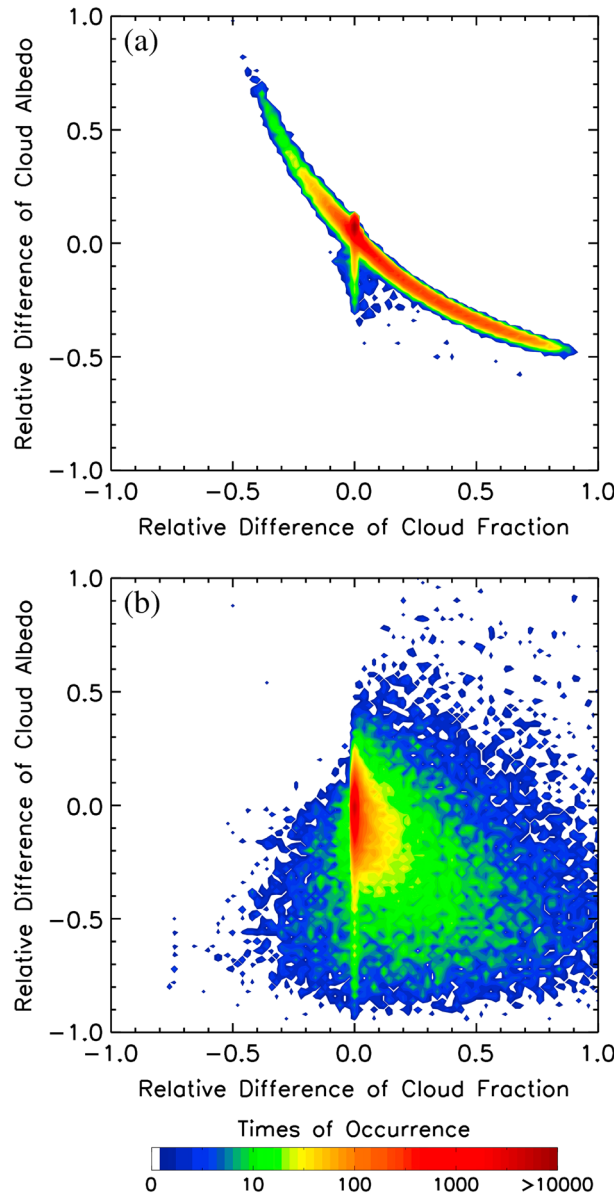


Figure 8. Comparisons between (a) RDA between Liu2011 and XL2013 and RDF between Long2006 and XL2013 and (b) RDA and RDF between Min2008 and XL2013.

when $f(\text{Long2006}) < f(\text{XL2013})$ as shown in Figure 6c. Thus, the above mentioned difference should be related to other source of uncertainties.

4.4. Mutual Contamination of Retrieval Errors

The preceding analysis shows that compared to Liu2011, XL2013 tends to have larger, smaller, and similar cloud albedo when the corresponding cloud fraction is smaller, larger, and similar compared to Long2006, respectively. This result suggests the possibility of mutual contamination of errors in retrievals of cloud fraction and cloud albedo; that is, any error in the retrieval of one quantity could lead to error in the other.

To further understand the potential problem of mutual error contamination, we regrouped the cloud fractions in Figure 1 according to the median of cloud albedo, $\alpha_r(\text{XL2013}) = 0.63$, in all data. Figures 7a and 7b compare the cloud fractions when $\alpha_r(\text{XL2013}) \leq 0.63$ and $\alpha_r(\text{XL2013}) > 0.63$, respectively. When $\alpha_r(\text{XL2013}) \leq 0.63$, the cloud fractions retrieved by XL2013 are generally smaller than Long2006. It can be also found that the thick

To further understand the difference of the retrieval algorithms, we use Long2006 and XL2013 as an example. The cloud fractions of Long2006 and XL2013 are further investigated according to the partition of their values of RDF and land surface albedo. The blue, black, and red boxes in Figure 5a, containing 12,806, 37,542, and 928 scenarios, respectively, are corresponding to the areas where $0.2 < \text{RDF} < 1.0$ and $0.1 < \alpha_s < 0.35$, $-0.05 < \text{RDF} < 0.05$ and $0.05 < \alpha_s < 0.95$, and $-1.0 < \text{RDF} < -0.2$ and $0.1 < \alpha_s < 0.35$, respectively. In other words, the blue, red, and black boxes correspond to $f(\text{Long2006}) > f(\text{XL2013})$, $f(\text{Long2006}) < f(\text{XL2013})$, and $f(\text{Long2006}) \sim f(\text{XL2013})$, respectively.

Figure 6 shows the comparisons of cloud fractions and cloud albedos for observations within the blue, black, and red boxes of Figure 5a. It is evident that most of the clouds related to $f(\text{Long2006}) > f(\text{XL2013})$ are optically thin (Figures 6a and 6d), whereas most clouds related to $f(\text{Long2006}) < f(\text{XL2013})$ have small cloud fractions are optically thick (Figures 6c and 6f). For clouds with similar cloud fractions from Long2006 and XL2013 (Figures 6b and 6e), the differences between the Liu2011 and XL2013 albedo retrievals are much smaller, especially considering that neglected effects from land surface albedo and cloud absorption in Liu2011 may cause biases as discussed earlier in section 4.2, which cannot be explained by different observational conditions and cloud structures discussed above. Moreover, the difference in observational conditions and cloud structures cannot explain clouds

clouds (Figure 7b) are typically identified as overcast conditions by both XL2013 and Long2006. In contrast to the thin clouds shown in Figure 7a, XL2013 gives larger cloud fractions for the thick clouds. The least squares fitting of Figures 7a and 7b indicates that the increase of thick clouds is much smaller than the decrease related to thin clouds when XL2013 is used in the retrieval, suggesting that on average, the cloud fraction from XL2013 is smaller than Long2006, consistent with what is shown in Figure 3. Figures 7a and 7b also suggest that the empirical formulation (i.e., equation (2)) of Long2006 is associated with the median of cloud albedo because it leads to the best match of the cloud fractions from XL2013 and Long2006. The median of cloud albedo should minimize the total uncertainty of retrieved cloud fraction when realistic cloud albedo is not considered in the retrieval.

Figures 7c and 7d compare the cloud albedos when cloud fraction, $f(\text{XL2013})$, is smaller or greater, respectively, than its median value 0.45. For a small cloud cover (Figure 7c), most of the cloud albedos associated with XL2013 are greater than Liu2011 due to the relationship of equation (4c) and the smaller cloud fraction by XL2013 shown in Figure 7a. The cloud albedo by XL2013 becomes smaller than Liu2011 when the cloud is thick, which is caused by the greater cloud fraction of XL2013 when $f(\text{XL2013}) < 0.1$. It is obvious from Figure 7d that the cloud albedos based on the two algorithms have excellent agreement when the cloud fraction is large. This can be explained by equation (4c) and the increasingly better agreement with cloud fraction in Figure 7a.

The effect of mutual contamination of retrieval errors can be also seen in the relationship between RDF and RDA (Figure 8). Figure 8a compares the RDF between Long2006 and XL2013 with RDA between Liu2011 and XL2013. It is clear that positive RDF is associated with negative RDA and vice versa. In comparison, the effect of mutual contamination can be also seen for most of the data of Min2008 and XL2013, although the negative correlation is less obvious. Less effect is understandable because the cloud albedo of Min2008 is based on separate retrieval of cloud optical thickness while that of Liu2011 and XL2013 is derived using the relationship between relative cloud forcing and cloud albedo.

5. Concluding Remarks

This study examines the retrieval techniques and results in the retrieval of cloud fraction and cloud albedo using surface-based SW broadband and spectral radiation measurements. The cloud fraction and cloud albedo obtained from Long2006 and Liu2011, respectively, are compared with a newly developed approach reported by XL2013 using 16 years of surface-based broadband radiation measurements collected at the ARM SGP site. The retrievals of XL2013 are further compared with those developed by Min2008 using spectral radiation measurements. The comparison shows that although the different retrievals have a good overall agreement, there are noticeable differences. Inspection of the differences shows that the cloud fractions of XL2013 are smaller than Long2006 for small cloud cover scenarios. The difference decreases with increasing cloud fraction. Compared to XL2013, Min2008 also produces larger cloud fractions. For thin clouds, the retrieved cloud albedos by XL2013 are greater than Liu2011 whereas the cloud albedos of XL2013 are smaller than Liu2011 for relatively thick clouds. The latter is likely due to the correction of cloud absorption in XL2013.

The diurnal, annual, and interannual variations of cloud albedo retrieved by Min2008 have similar pattern to Liu2011 and XL2013 but with smaller values. Conversely, the relative magnitudes of the cloud fractions based on the Min2008 and XL2013 approaches are opposite those of cloud albedos. The overall mean cloud fractions of Long2006, Min2008, and XL2013 are all greater than other surface and satellite measurements due to the exclusion of the data related to small cloud covers.

Compared to XL2013, the neglect of land surface albedo by Liu2011 and different observational conditions and cloud structures by Long2006 have limited contributions to the differences in the retrieval of cloud albedo and cloud fraction, respectively. It is discovered that the cloud fractions of XL2013 are smaller and greater than Long2006 for thin and thick clouds, respectively. The empirical formulation of Long2006 is likely associated with a fixed cloud albedo. The cloud albedo of Liu2011 and XL2013 has a good agreement for large cloud covers, which is related to their better agreement of cloud fractions from Long2006 and XL2013. These results suggest that the mutual contamination of errors in retrievals of cloud fraction and cloud albedo may be a major source of the difference between the retrievals.

A few points are noteworthy for future study. First, this study examines the performance of different retrieval algorithms on the estimates of cloud fraction and cloud albedo over the ARM SGP site. Similar analyses can be

conducted using data collected at other regions such as the ARM site at the North Slope Alaska to improve understanding of the retrieval algorithms. Second, both Liu2011 and XL2013 use the assumption of plane-parallel assumption in the simulation of radiation transfer. This assumption may cause errors in the retrievals, especially for small clouds with strong 3-D effects [Marshak and Davis, 2005]. Third, this study focuses on surface-based retrievals. The satellite measurements of the top-of-atmosphere fluxes can be combined with surface measurements to estimate cloud thermodynamic phase and cloud absorption in the simultaneously retrieval of cloud fraction and cloud albedo. Compared to the use of previously estimated cloud absorption by XL2013, this simultaneous retrieval should further improve the accuracy of cloud fraction and cloud albedo. Finally, the differences in the definition of cloud fraction and cloud albedo between GCMs and observations have been an outstanding issue in model evaluation against measurements [Kassianov et al., 2005]. The use of the total radiation partitioned into direct and diffuse radiation in retrievals holds great promise for having a comparison between cloud fraction and cloud albedo simulated by GCMs and observations in a consistent way.

Acknowledgments

This work is supported by the U.S. Department of Energy's Earth Systems Modeling (ESM) program via the FASTER project (www.bnl.gov/faster), Office of Biological and Environmental Research, and the Atmospheric Systems Research (ASR) Program. The work uses data from the Atmospheric Radiation Measurement (ARM) Climate Research Facility (<http://www.arm.gov/data/vaps/swfluxanal>).

References

- Betts, A. K. (2007), Coupling of water vapor convergence, clouds, precipitation, and land-surface processes, *J. Geophys. Res.*, *112*, D10108, doi:10.1029/2006JD008191.
- Betts, A. K., and P. Viterbo (2005), Land-surface, boundary layer, and cloud-field coupling over the southwestern Amazon in ERA-40, *J. Geophys. Res.*, *110*, D14108, doi:10.1029/2004JD005702.
- Bouniol, D., et al. (2010), Using continuous ground-based radar and lidar measurements for evaluating the representation of clouds in four operational models, *J. Appl. Meteorol. Clim.*, *49*(9), 1971–1991.
- Charlock, T. P., and V. Ramanathan (1985), The albedo field and cloud radiative forcing produced by a general-circulation model with internally generated cloud optics, *J. Atmos. Sci.*, *42*(13), 1408–1429.
- Dong, X. Q., P. Minnis, and B. K. Xi (2005), A climatology of midlatitude continental clouds from the ARM SGP Central Facility: Part I: Low-level cloud macrophysical, microphysical, and radiative properties, *J. Clim.*, *18*(9), 1391–1410.
- Dong, X. Q., B. K. Xi, and P. Minnis (2006), A climatology of midlatitude continental clouds from the ARM SGP central facility. Part II: Cloud fraction and surface radiative forcing, *J. Clim.*, *19*(9), 1765–1783.
- Gautier, C., and M. Landsfeld (1997), Surface solar radiation flux and cloud radiative forcing for the atmospheric radiation measurement (ARM) southern great plains (SGP): A satellite, surface observations, and radiative transfer model study, *J. Atmos. Sci.*, *54*(10), 1289–1307.
- Han, Q. Y., W. B. Rossow, J. Chou, and R. M. Welch (1998), Global survey of the relationships of cloud albedo and liquid water path with droplet size using ISCCP, *J. Clim.*, *11*(7), 1516–1528.
- Harrison, L., J. Michalsky, and J. Berndt (1994), Automated multifilter rotating shadow-band radiometer: An instrument for optical depth and radiation measurements, *Appl. Opt.*, *33*(22), 5118–5125.
- Henderson-Sellers, A., and K. Mcguffie (1990), Are cloud amounts estimated from satellite sensor and conventional surface-based observations related?, *Int. J. Rem. Sens.*, *11*(3), 543–550.
- Hinkelman, L. M., T. P. Ackerman, and R. T. Marchand (1999), An evaluation of NCEP Eta model predictions of surface energy budget and cloud properties by comparison with measured ARM data, *J. Geophys. Res.*, *104*(D16), 19,535–19,549, doi:10.1029/1999JD900120.
- Hogan, R. J., C. Jakob, and A. J. Illingworth (2001a), Comparison of ECMWF winter-season cloud fraction with radar-derived values, *J. Appl. Meteorol. Clim.*, *40*(3), 513–525.
- Hogan, R. J., C. Jakob, and A. J. Illingworth (2001b), Comparison of ECMWF winter-season cloud fraction with radar-derived values, *J. Appl. Meteorol.*, *40*(3), 513–525.
- Kassianov, E., C. N. Long, and M. Ovtchinnikov (2005), Cloud sky cover versus cloud fraction: Whole-sky simulations and observations, *J. Appl. Meteorol.*, *44*(1), 86–98.
- Kennedy, A. D., X. Dong, and B. Xi (2013), Cloud fraction at the ARM SGP site, *Theor. Appl. Climatol.*, doi:10.1007/s00704-00013-00853-00709.
- Lazarus, S. M., S. K. Krueger, and G. G. Mace (2000), A cloud climatology of the Southern Great Plains ARM CART, *J. Clim.*, *13*, 1762–1775.
- Liu, Y. G., W. Wu, M. Jensen, and T. Toto (2011), Relationship between cloud radiative forcing, cloud fraction and cloud albedo, and new surface-based approach for determining cloud albedo, *Atmos. Chem. Phys.*, *11*, 7155–7170.
- Long, C., and T. P. Ackerman (2000), Identification of clear skies from broadband pyranometer measurements and calculation of downwelling shortwave cloud effects, *J. Geophys. Res.*, *105*(D12), 15,609–15,626, doi:10.1029/2000JD900077.
- Long, C., and K. L. Gaustad (2004), The shortwave (SW) clear-sky detection and fitting algorithm: Algorithm operational details and explanations, *Atmos. Rad. Meas. Prog. Tech. Rep.*, 26 pp.
- Long, C., T. P. Ackerman, K. L. Gaustad, and J. N. S. Cole (2006), Estimation of fractional sky cover from broadband shortwave radiometer measurements, *J. Geophys. Res.*, *111*, D11204, doi:10.1029/2005JD006475.
- Marshak, A., and A. B. Davis (2005), *3D Radiative Transfer in Cloudy Atmospheres*, 701 pp., Springer, Heidelberg.
- McFarlane, S. A., C. N. Long, and J. Flaherty (2013), A climatology of surface cloud radiative effects at the ARM tropical western Pacific sites, *J. Appl. Meteorol.*, *52*(4), 996–1013.
- Min, Q., and L. C. Harrison (1996), Cloud properties derived from surface MFRSR measurements and comparison with GOES results at the ARM SGP site, *Geophys. Res. Lett.*, *23*(13), 1641–1644, doi:10.1029/96GL01488.
- Min, Q., E. Joseph, and M. Z. Duan (2004), Retrievals of thin cloud optical depth from a multifilter rotating shadowband radiometer, *J. Geophys. Res.*, *109*, D02201, doi:10.1029/2003JD003964.
- Min, Q., T. Wang, C. N. Long, and M. Duan (2008), Estimating fractional sky cover from spectral measurements, *J. Geophys. Res.*, *113*, D20208, doi:10.1029/2008JD010278.
- Minnis, P., et al. (2008), Near-real time cloud retrievals from operational and research meteorological satellites, paper presented at Proc. SPIE European Remote Sensing, International Society for Optics and Photonics, Cardiff, Wales, UK, 15–18 September.
- Mlawer, E. J., S. J. Taubman, P. D. Brown, M. J. Iacono, and S. A. Clough (1997), RRTM, a validated correlated-k model for the longwave, *J. Geophys. Res.*, *102*, 16,663–16,682, doi:10.1029/97JD00237.

- Ohmura, A., et al. (1998), Baseline Surface Radiation Network (BSRN/WCRP): New precision radiometry for climate research, *Bull. Am. Meteorol. Soc.*, 79(10), 2115–2136.
- Oreopoulos, L., and H. W. Barker (1999), Accounting for subgrid-scale cloud variability in a multi-layer 1-D solar radiative transfer algorithm, *Q. J. Roy. Meteorol. Soc.*, 125, 301–330.
- Paquin-Ricard, D., C. Jones, and P. A. Vaillancourt (2010), Using ARM observations to evaluate cloud and clear-sky radiation processes as simulated by the Canadian regional climate model GEM, *Mon. Weather Rev.*, 138(3), 818–838.
- Qian, Y., C. N. Long, H. Wang, J. M. Comstock, S. A. McFarlane, and S. Xie (2012), Evaluation of cloud fraction and its radiative effect simulated by IPCC AR4 global models against ARM surface observations, *Atmos. Chem. Phys.*, 12(4), 1785–1810.
- Sagan, C., and J. B. Pollack (1967), Anisotropic nonconservative scattering and the clouds of Venus, *J. Geophys. Res.*, 72, 469–477, doi:10.1029/JZ072i002p00469.
- Sengupta, M., E. E. Clothiaux, and T. P. Ackerman (2004), Climatology of warm boundary layer clouds at the ARM SGP site and their comparison to models, *J. Clim.*, 17(24), 4760–4782.
- Song, H., W. Y. Lin, Y. L. Lin, A. B. Wolf, R. Neggers, L. J. Donner, A. D. Del Genio, and Y. G. Liu (2013), Evaluation of precipitation simulated by seven SCMs against the ARM observations at the SGP site, *J. Clim.*, 26(15), 5467–5492.
- Warren, S. G., C. J. Hahn, J. London, R. M. Chervin, and R. L. Jenne (1986), Global distribution of total cloud cover and cloud type amounts over land, *NCAR Tech. Note NCAR/TN-273+STR*, Natl. Cent. for Atmos. Res., Boulder, Colo.
- Wigley, T. M. L., P. D. Jones, K. R. Briffa, and G. Smith (1990), Obtaining sub-grid-scale information from coarse-resolution general-circulation model output, *J. Geophys. Res.*, 95(D2), 1943–1953, doi:10.1029/JD095iD02p01943.
- Wu, W., Y. G. Liu, M. P. Jensen, T. Toto, M. J. Foster, and C. N. Long (2014), A comparison of multiscale variations of decade-long cloud fractions from six different platforms over the Southern Great Plains in the United States, *J. Geophys. Res. Atmos.*, 119, 3438–3459, doi:10.1002/2013JD019813.
- Wyant, M. C., M. Khairoutdinov, and C. S. Bretherton (2006), Climate sensitivity and cloud response of a GCM with a superparameterization, *Geophys. Res. Lett.*, 33, L06714, doi:10.1029/2005GL025464.
- Xie, Y., and Y. G. Liu (2013), A new approach for simultaneously retrieving cloud albedo and cloud fraction from surface-based shortwave radiation measurements, *Environ. Res. Lett.*, 8, doi:10.1088/1748-9326/1088/1084/044023.
- Zhang, M. H., et al. (2012), CGILS: Results from the first phase of an international project to understand the physical mechanisms of low cloud feedbacks in single column models, *J. Adv. Model. Earth Syst.*, 4, 826–842, doi:10.1029/2012MS000182.